

## **GEOLOGY AND GEOCHEMISTRY OF AL FAWAKHIR MINING DISTRICT, CENTRAL EASTERN DESERT, EGYPT**

**<sup>1</sup>Sharaky, A.M., <sup>2</sup>Oweiss, Kh.A., <sup>1</sup>Abdel Maksoud, K.M.**

**<sup>1</sup>Department of Natural Resources, Institute of African Research and  
Studies, Cairo University, Giza 12613, Egypt**

**<sup>2</sup>Egyptian Mineral Resources Authority**

### **ABSTRACT**

Al Fawakhir mining district lies in rugged Precambrian mountains of the Central Eastern Desert. It is almost exactly halfway between the Qift, Nile Valley and Quseir, Red Sea. It comprises two gold mines Al Fawakhir and Al Sid. The study area is located between latitudes 25° 57' 00" and 26° 00' 00" N and longitudes 33° 35' 00" and 33°33'30" E, covering about 120 km<sup>2</sup>. The mining processes in Al Fawakhir area started early during the Pharaonic time. The mine was working early in the last Century up to 1958. A geologic map to the scale of 1:40,000 was reconstructed based on Landsat enhanced thematic mapper (ETM<sup>+</sup>) image and aerial photographs with comprehensive fieldwork during February 2007. Al Fawakhir district is mainly covered by basement peridotite rocks including the oldest rocks of metamorphic ophiolites (serpentinites) followed by metagabbros, granitic rocks, Dokhan Volcanics and the youngest doleritic dykes and quartz veins.

Native gold was recorded in the main quartz veins. Silicification is common along both sides of the shear zones, reflecting the effect of hydrothermal solutions mostly derived from the younger granitic intrusions. It is associated with ore sulfide minerals and native gold. Pyrite is the most predominant sulfide mineral in the veins followed by arsenopyrite. Other subordinate sulfides include sphalerite, chalcopyrite, pyrrhotite and galena.

The geochemical analyses of 15 whole rock samples collected from ophiolitic and granitic rocks were carried on for major oxides and some trace elements including Rb, Ta, Hf, Sr, Nb and Y to investigate the geochemical conditions of the country rocks that host gold-bearing quartz veins. The geochemical analyses, petrochemical calculations, and plotting on the international binary and ternary diagrams revealed that the metamorphic peridotites belong to the metamorphic dunite, and lherzolite associated with ophiolites. The metagabbros are of tholeiitic nature and are of the cumulate type. The granitic rocks are of subalkaline to alkaline nature.

### **INTRODUCTION**

The area under investigation lies within the Basement Complex of the Central Eastern Desert of Egypt. It is located along the asphalt road between Quseir and Qift. Two gold mines are known in the area, Al Fawakhir and Al Sid gold mines. Al Sid mine is located at 78 km from Quseir, while Al Fawakhir mine is located at another 4 km to the northwest at Bir Al Fawakhir. This area occurs at the northern central part of the Central Eastern Desert of Egypt (Fig. 1). The study area lies between latitudes 25° 57' 00" and 26° 00' 00" N and longitudes 33° 35' 00" and 33° 38' 30" E, covering about 62.5 km<sup>2</sup>. It is one of the largest mesothermal vein-type gold deposits in the Eastern Desert of Egypt (Hume 1937; Harraz et al., 1992, Harraz, 2000), which are mainly hosted in the Pan-African granites of 590 to 585 Ma (Meneisy and Lenz, 1982) or 620 to 570 Ma (Hassan and Hashad, 1990).

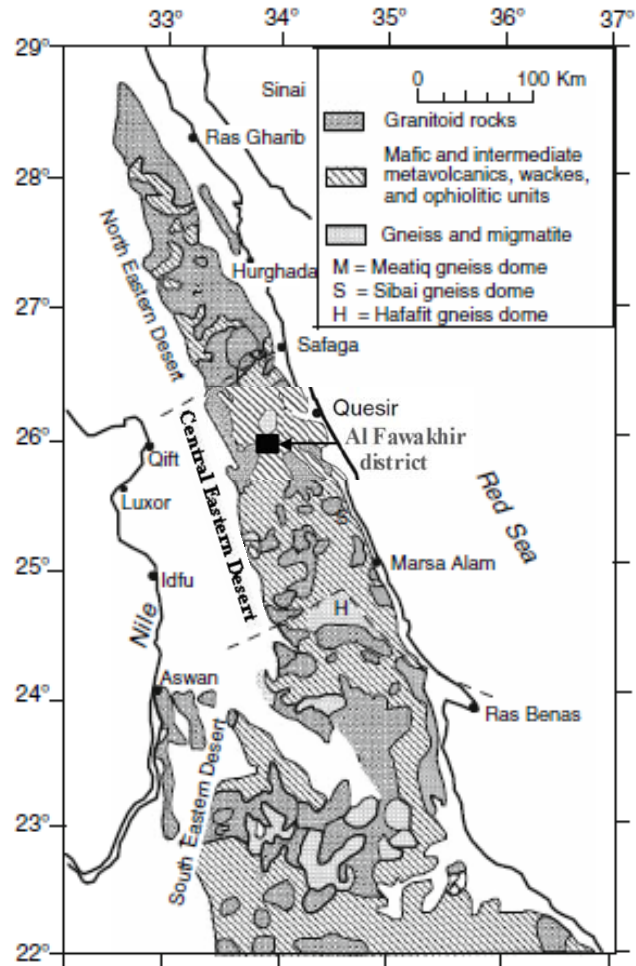


Figure 1: Regional geologic map of the Eastern Desert, Egypt. Modified by Andresen et al. (2009) from Moussa et al. (2007). The solid rectangle represents the study area of Al Fawakhir district.

The Eastern Desert has been well known as a gold-mining area since Ancient Egyptians (Enoch, 1999, Klemm et al. 2001; Botros, 2004) and more than 90 gold deposits and occurrences (Botros, 2004). The present work deals with the geology and geochemistry of Al Fawakhir mining area and investigates the field crosscutting relationships of gold-bearing quartz veins with the country rocks to infer the origin of mineralizing fluids.

Many of the gold localities in Egypt were intensively mined, particularly during the Pharaonic and Roman times and the mines were exploited at various times until 1958. At the beginning of the last century, the majority of these gold mines were re-evaluated and exploited. A stage of gold exploration and production had been started in the Eastern Desert during the period between 1933 and 1958 particularly in Al Sid and Al Fawakhir gold mines. According to Kochin and Bassyuni (1968) the gold content of the exploited deposits during that period ranged between 11 and 30 g/ton and the total gold production from 1902 to 1958 was about 6.93 tons. The oldest geologic map (on papyrus) illustrating mine features is that of King Siti I (1,350-1,205 B.C.) for Al Fawakhir mine. The map was discovered in 1820 A.C. and now kept in the Egyptian Museum in Torino, Italy (Afia, 1984).

The present work is carried out to state clear and definite field relations between the different rock groups recorded in Al Fawakhir area. This is done through mapping and comprehensive field work, in addition to analysis of the observed structural elements.

## LOCAL GEOLOGY

The Central Eastern Desert is occupied by Precambrian crystalline rocks that comprise gneisses, schists, metagabbros, metasediments and ophiolites. They are intruded by syn-orogenic and post-orogenic granitoids and their associated calc-alkaline volcanics (Dokhan Volcanics).

Al Fawakhir area is covered by dismembered masses of serpentinites, metavolcanics, metagabbros and synorogenic calc-alkaline granites. Boulgatov et al. (1980) described the different rock units encountered in a regional sector including the study area. They produced a geologic map (scale of 1:10,000) for limited- prospecting area, south Al Sid gold mine. Panning, metallometric and channel sampling were done. El Gaby (1983) published a Quseir regional geologic map of the Hammamat-Quseir region, simplified and modified from the geological map of Qena and Aswan quadrangles.

Using satellite imagery and aerial photographs the examined area was mapped through comprehensive field work. A geologic map to the scale 1:40,000 is given in Figure 2. Field work, sampling, reveals that the investigated area is covered by basement rocks arranged from younger to the older: Quartz veins - Doleritic dykes- Dokhan Volcanics- Granitic rocks Metagabbros.

### Metamorphic Peridotites

#### Metamorphic peridotites (serpentinites):

The metamorphic peridotites (serpentinites) form a host aureole intruded by all the other rock units of the study area (Fig. 2). The serpentinites are intruded by the metagabbros which interns are intruded by the pink granites at the central part of the mapped area (Fig. 3a). The metagabbros caught up major xenolithic (Fig. 3b) masses of the metamorphic peridotites. The pink granites intrude the serpentinites forming peculiar green masses spotted with pink patches. The serpentinite boulders engulfed by the pink granites are covered by buff weathered tarnish formed after thin granitic filament.

#### Metagabbros:

The field observations were found to be the more effective criteria for the distinction among these gabbroic rocks (Fig. 2). The ophiolitic metagabbros occur as layered and cumulate masses in the ophiolitic successions widespread in the Central and South Eastern Desert. They represent pieces of oceanic crust obducted along destructive plate boundaries during the closure of small ocean basin. The successions are commonly located along major thrust faults (Hassanien, 1978) the metagabbros intrude the serpentinites forming several mappable units. Frequently, they form unmappable xenoliths masses within the southern part of the granitic mass. The metagabbros are intruded by the pink granites with sharp and intrusive contact (Fig. 3c).

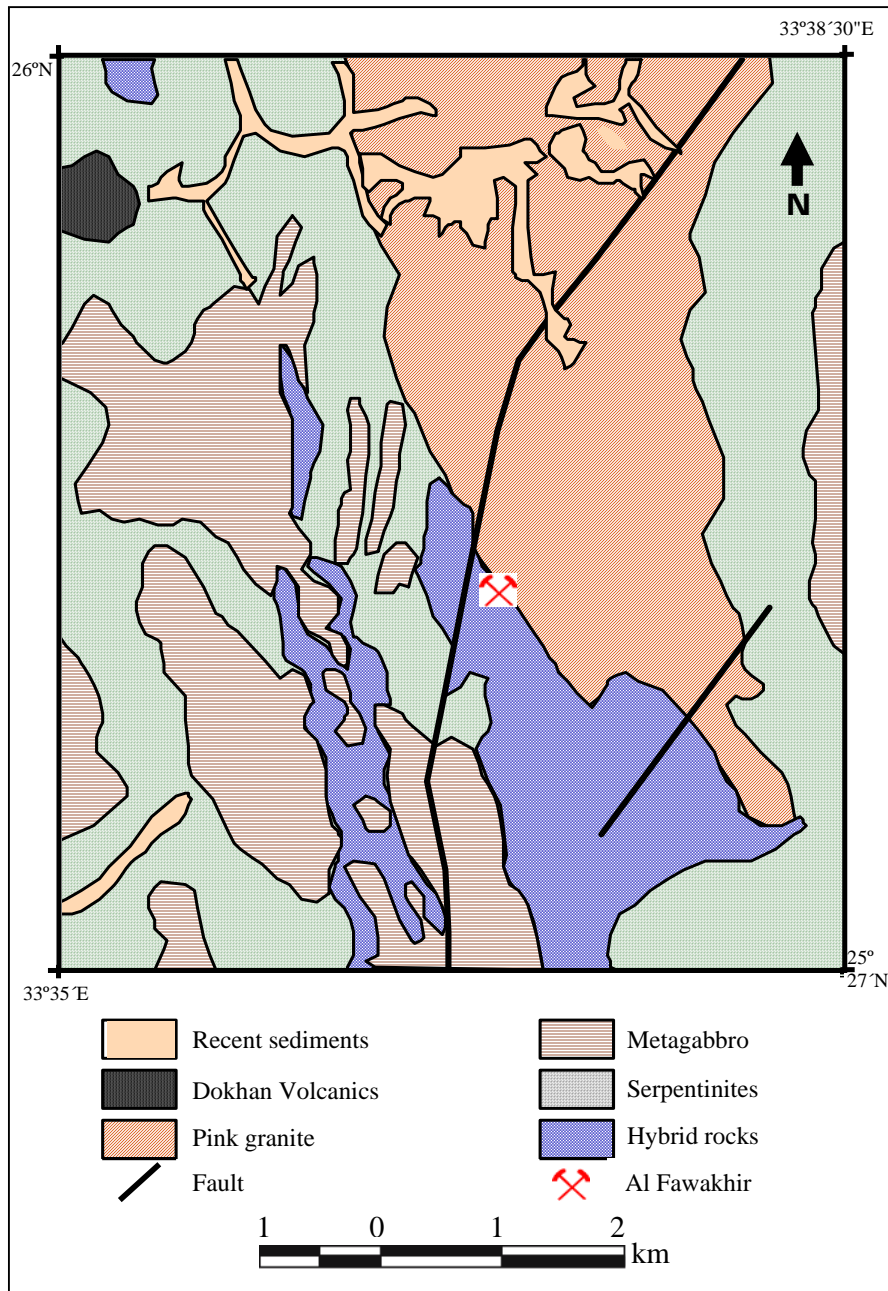


Figure 2. Geologic map of the Al Fawakhir mining district.



**Figure 3. Field photographs for the Al Fawakhir mining district.**

- a. Panoramic view along Qusier-Qift Road in the study area showing sequence of serpentinite (Ser), metagabbro (MG) and pink granite (PG). Looking East.**
- b. Metagabbro caught up a big xenolithic mass of serpentinite (Sp).**
- c. Contact between pink granite (PG) and metagabbro (MG). Looking South.**
- d. Major xenolithic mass of metagabbro (MG) showing boundary weathering in the main granitic mass (PG) of the gold mine site. Looking SW.**
- e. Columnar jointing forms in Dokhan Volcanics.**
- f. Doleritic dike intruded in pink granite (PG). Looking South.**
- g. Hydrothermal alteration halo along quartz vein at Al Sid gold mine.**

### **Granitic rocks:**

More than 40% of the Egyptian Basement Complex is covered by granitic rocks of different composition and varying tectonic set-up. Several trials were made aiming at the establishment of a satisfactory classification of these granites. Since Hume (1935), up to the present time, workers on the Basement Complex agree that the younger granites constitute 16.2% of the basement outcrops in the Eastern Desert. Akaad and El Ramly (1960) were the first to use this term of older and younger granites in classification. Meneisy (1972) and Hashad (1980) stated that the age of the younger granite ranges from 568 to 594 Ma, which represents a restricted span of time during the Pan-African events. The granitic rocks occupy the central part of the study area (Fig. 2). The main complex consists of two masses, northern mass of pure granitic composition and southern mass frequently spotted with metagabbroic xenoliths that are unmapable to the present scale of mapping (Fig. 3d).

A highly hybrid zone of nearly granitic composition stretches parallel to the main mass, to the west. Along this stretch several mapable units of metagabbro are clearly observed and are aligned (NNW) parallel to the long axis of the main granitic mass. The granitic complex of the study area is emplaced along three magmatic phases (Boulgatov et. al., 1980). The pink granites intrude sharply the metamorphic peridotites and the metagabbros and are traversed by late basic dykes and quartz veinlets. Three phases of intrusion are conventionally discriminated in the development of the present Al Fawakhir granitic rocks. The frequent occurrence of undigested metagabbro all over the granitic complex indicates that the granitic magma was acting as heat engine on the mafic- ultra mafic complex of this particular area. The granitic rocks are highly jointed. Closely spaced master joints are frequently observed. These sets of normal joints usually separate rectangular blocks.

### **Dokhan Volcanics:**

The Dokhan Volcanics constitute a small mass located at the extreme north western part of the study area (Fig. 2). Dokhan Volcanics consist of a thick sequence of stratified lava flows of intermediate to acidic composition, together with subordinate sheets of ignimbrites and intercalations of pyroclastics and siltstones. These rocks have different shades of gray that frequently grade into reddish color. The rocks are highly jointed with narrow joint system (Fig. 3e).

### **Late Doleritic Dykes:**

Doleritic dykes ranging between 0.5 and 1.5 m in thickness traverse all the previously mentioned rock units with sharp contact (Fig. 3f)

### **Veins:**

The study area is traversed by gold-bearing quartz veinlets. The main occurrences are those at Al Fawakhir and El Sid mine area where main quartz veins are exploited for gold. These quartz veinlets represent the second stage of the heat engine process affecting the area and lead to the accumulation of gold along two stages of formation. The first stage accompanied the granitic intrusion where the mafic ultramafic rocks were heated and gold was mobilized to the heat source. The second stage is the intrusion of these quartz veinlets. The ore bodies of the vein type represent fissure fillings with some wall rock alterations in their vicinity (Fig. 3g).

### **Faults:**

The Al Fawakhir gold mine area suffered from different tectonic events Benjamin et al. (2005). Faults are observed through apparent displacement of late dykes, and or lithologic contacts, as well as through the presences of slickensided surface. Faults are displacing each other as they occurred during different periods of tectonic activity. (1) Initial west verging thrusting of ophiolite nappes was followed by the formation of a conjugate strike slip shear zone system. (2) Subsequently the conjugate shear zone formed pull-part structures in which the Al Fawakhir granites were intruded. (3) During the late stage of deformation, extensional tectonics and normal faulting occurred and East-West striking extensional quartz veins were built.

## **PETROGRAPHY**

### **Metamorphic peridotites**

The metamorphic peridotites represent the basal part of the sequence and include dunite serpentinite and lherzolite serpentinites. The dunite serpentinite is composed chiefly of antigorite, lizardite, chrysotile with accessory of pseudomorph bastite structure and iron oxides (Fig. 4a). Lherzolite-serpentinite consists dominantly of partially altered olivine, ortho-pyroxene, clino-pyroxene with minor amounts of talc and accessory amounts of iron oxide (Fig. 4b).

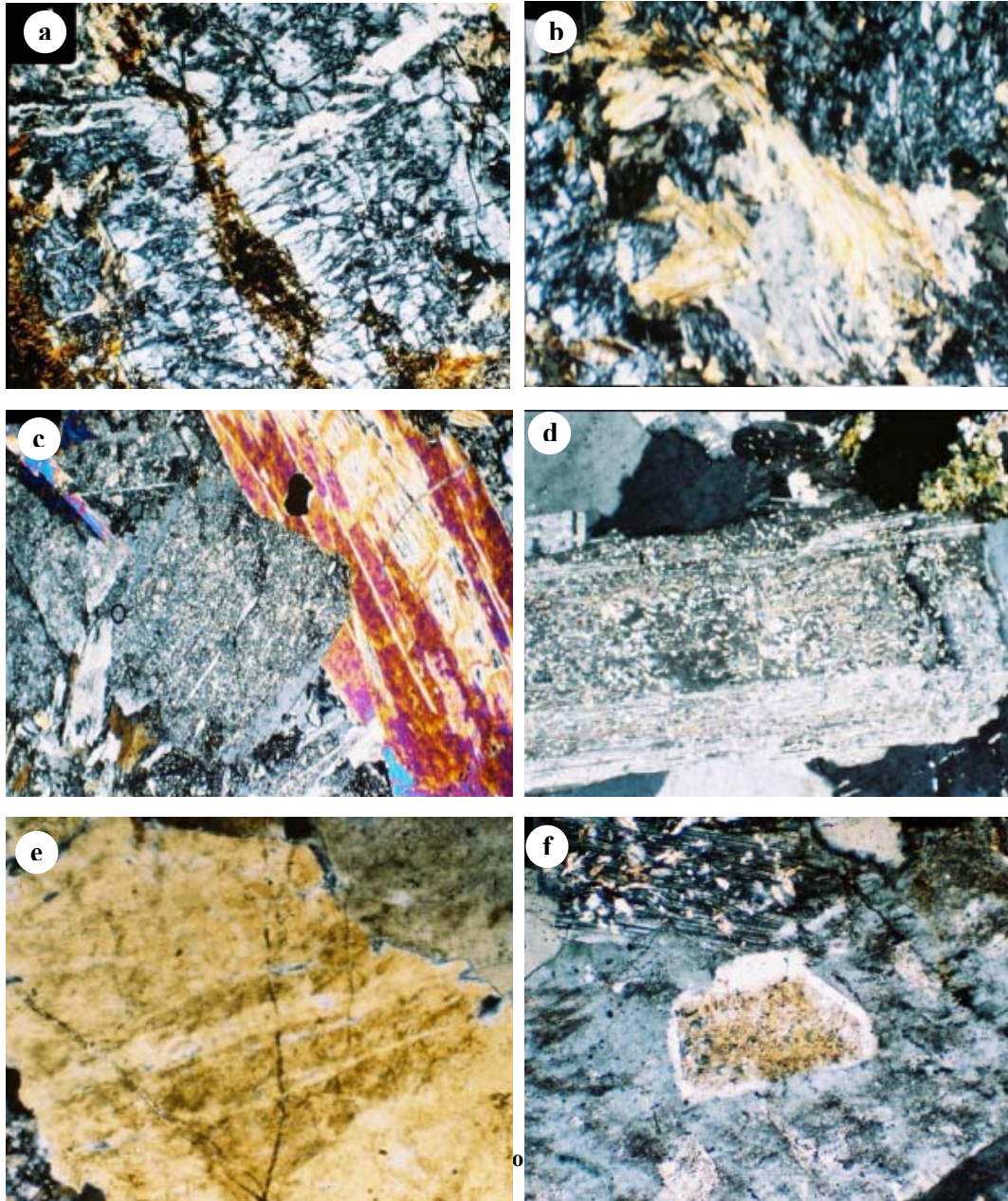
### **The metagabbros**

The metagabbro complex includes the layered cumulate varieties as well as the massive metagabbro. Microscopically, the rock is fine to coarse grained with hybridomorphic texture, consisting essentially of altered hornblende, saussuritized plagioclase, mafics and accessory iron-oxides (Fig. 4c).

### **Granitic rocks**

Modal analysis was carried out on 9 samples of granitic rocks of Al Fawakhir area (Table 1), using an automatic electric counter. Quartz, alkali feldspars, plagioclase, mafics and opaques are the counted components (Fig. 5), the classification diagram of Streckeisen (1967), shows that the examined granites are monzogranites, syeno-granites and alkali feldspar granites. Broadly speaking, alkali feldspar granites are associated with alkali feldspar syenites, syenites and monzonites. This series of granitoids and associated rocks which lie parallel to, and above, the silica saturation line A-P are located in areas of continental rifting (Bonin, 1980).

Plotting the 9 samples on the QAP diagram (Fig. 6) shows that all the examined samples are located in the field of granitoids formed by crustal fusion. The monzogranite consists mainly of K-feldspar and quartz with less abundant plagioclase and ferromagnesian minerals. The accessory minerals are apatite, zircon, sphene and opaques. The ferromagnesian minerals are hornblend and biotite. The texture is equigranular alltroimorphic texture (Fig. 4d).



- a. Antigorite veinlet intruding the dunite serpentinite. C.N. X80.
- b. Orthopyroxene (enstatite) dissected by fibrous serpentinite. Liherzolite serpentinite C.N. X80.
- c. Saussoritized plagioclase showing spots of minute epidotocrystals. Metagabbro C.N. X80.
- d. Sericitic alteration in plagioclase. C.N. X80.
- e. Vein perthite in syenogranite. C.N. X80.
- f. Perthite plate encloses corroded zoned plagioclase crystal. Alkaline granite C.N. X80.

Table 1: Modal data of Al Fawakhir pink granite.

Rock type	Syeno-granite			Monzogranite			Alkali granite		
	1	2	3	4	5	6	7	8	9
Quartz	35.00	16.50	25.75	31.70	30.50	32.60	35.30	34.70	35.00
Plagioclases	37.25	23.07	30.18	27.06	25.00	29.00	9.64	2.77	6.20
Alkali feldspars	24.25	38.84	23.68	38.72	37.00	30.40	26.07	54.86	40.30
Mafics	3.35	7.69	5.52	-	6.00	4.00	16.07	1.38	8.70
Opacues	-	18.94	14.00	2.25	2.00	4.00	12.14	6.09	9.30
Accessories	0.15	0.11	0.14	0.30	0.10	0.12	0.17	0.25	0.12
Total	100	100	100	100	100	100	100	100	100

The syeno-granite is medium- grained, with porphyritic texture consisting of orthoclase perthite, plagioclase, hornblende and biotite embedded in fine grained groundmass of K-feldspar and accessory quartz and apatite (Fig. 4e). The alkaline granite shows hypidiomorphic equigranular texture and consists mainly of quartz, perthitic K-feldspar, plagioclase and biotite. Iron oxides are accessories. Quartz forms anhedral to subhedral crystals. K-feldspar is mainly formed of perthite, forming subhedral crystals of ribbon and flame-types (Fig. 4f).

#### Hybrid rocks:

The hybrid rocks range between metagabbro and granite hornblende is intermixed with biotite and quartz in the interstitial spaces and along the cleavage planes of the plagioclase (Fig. 7a). Saussuritized plagioclase is in intimate association with quartz (Fig. 7b). It is clear that the metagabbros did not lose its mineral identity but it is highly affected by the hot granitic melt crystallized later along cracks, and cleavage planes of the metagabbros.

#### Quartz veins:

Quartz was formed during two phases of crystallization. Silica melt filled the interstitial spaces between subhedral to anhedral quartz plates (Fig. 7c). Sharara and Vennemann (1999) described 2 stages of quartz development. Stage I involves an intense silicification of the shear zones leading to the wide replacement of the Fe-bearing minerals of the host rocks and the deposition of auriferous sulfides on both sides of the shear zone. Stage II represents the main stage of filling of the dilatant sites of the shear zone by silica to form the main quartz veins.

Ore minerals are intruded along fractures in quartz veins. They are also recorded as irregular patches replacing the quartz groundmass. Pyrite is the most predominant sulfide mineral in the veins followed by arsenopyrite. Other subordinate sulfides include sphalerite, chalcopyrite, iron oxyhydroxide after pyrite, pyrrhotite and galena. Pyrite ( $\text{FeS}_2$ ) forms euhedral cubic crystals with sphalerite ( $\text{Zn,FeS}$ ) inclusions. Pyrite is frequently replaced by iron oxyhydroxide ( $\text{FeO}\cdot\text{OH}$ ) along cleavage planes. Native gold is observed in pyrite (Fig. 7d). Pyrite crystals are occasionally disposed in parallel alignment along the contact between quartz veins and the adjacent country rocks.

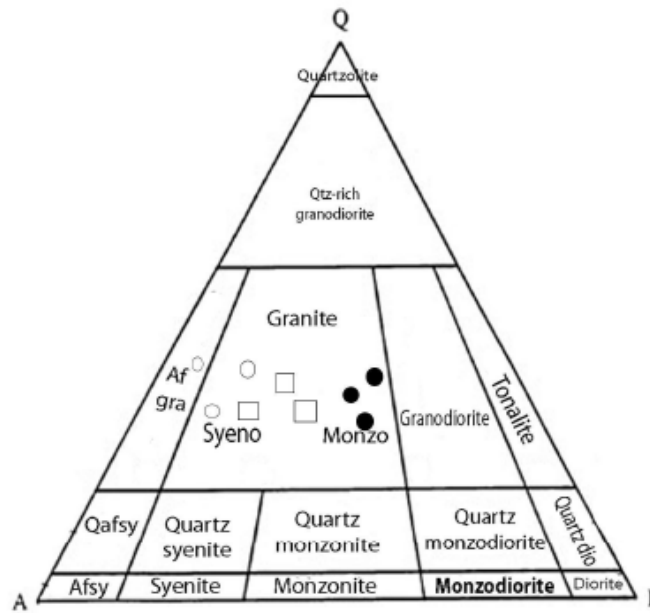


Figure 5. Streckeisen (1967) QAP (Quartz – Alkali feldspar – Plagioclase) diagram showing the trends in modal mineralogy of rocks from the Al Fawakhir mining district.

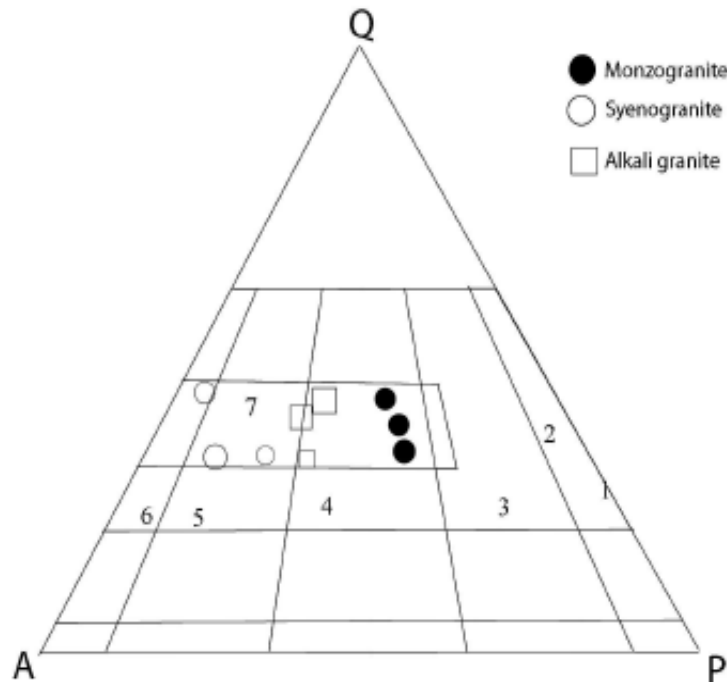


Figure 6. Streckeisen (1967) QAP (Quartz – Alkali feldspar – Plagioclase) diagram illustrating the trends in modal mineralogy of rocks from the Al Fawakhir mining district. The field determined granitoids formed by crustal fusion after Lameyre and Bowden (1982).

1. Tholeiitic 2. Calc-alkaline-trondhjemitic 3. Calc-alkaline-granodioritic 4. Calc-alkaline-monzonitic 5. Aluminous granitoids 6. Alkaline and peralkaline 7. Overlapping field of granitoids formed by crustal fusion.

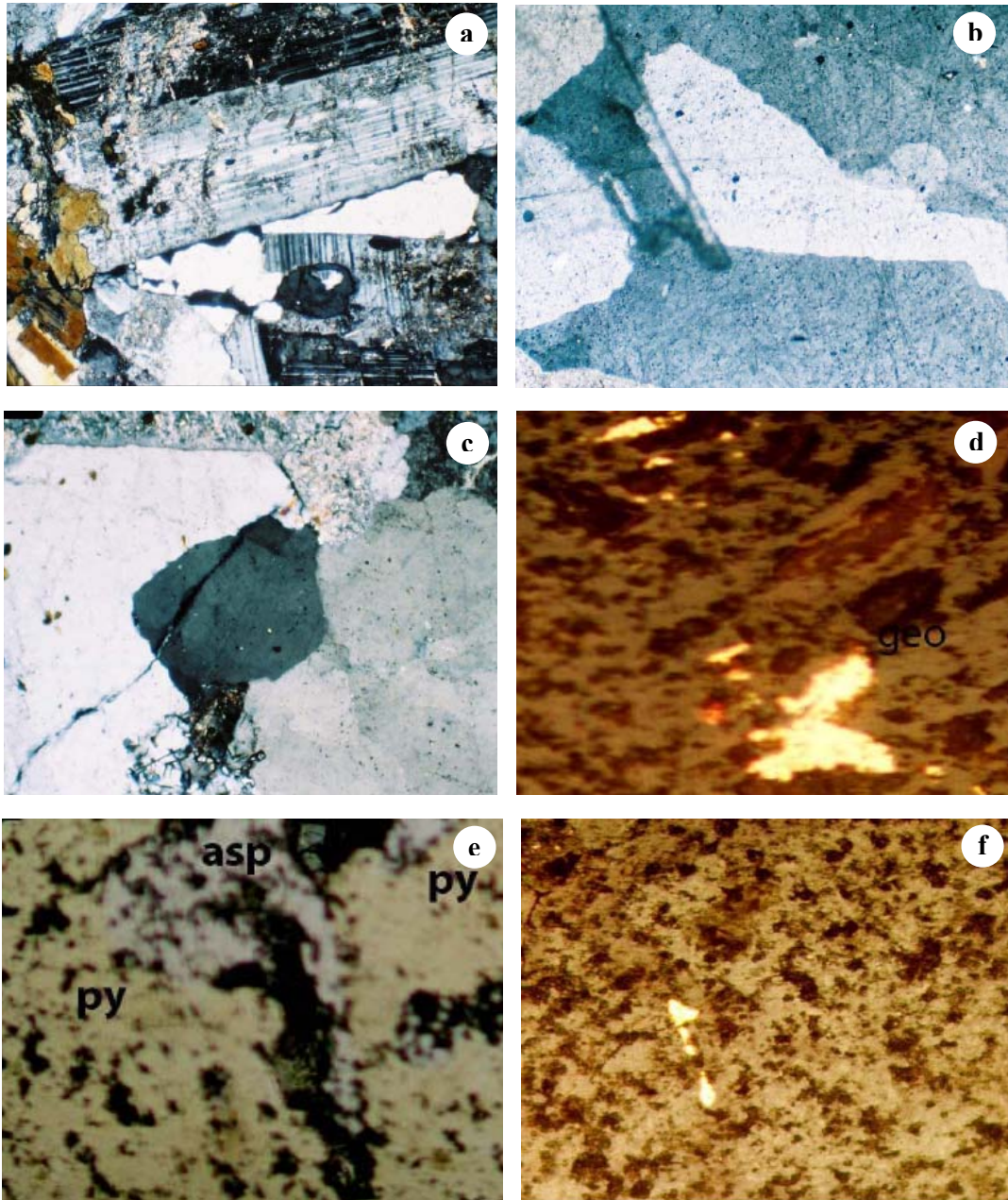


Figure 7. Photomicrographs of some studied samples.

- a. Hornblende and biotite occupying interstitial space between plagioclase crystals. Grano-Gabbro. C.N. X80.
- b. Saussuritized plagioclase of the metagabbro in intimate association with the quartz of the granitic rocks. Grano-gabbro C.N. X80.
- c. Two phases of quartz vein. C.N. X80.
- d. Geothite (geo) with native gold in quartz vein. Reflected light, C.N. X80.
- e. Patches of arsenopyrite (asp) in pyrite (py). Reflected light, C.N. X80.
- f. Native gold in quartz vein. Reflected light, C.N. X80.

Pyrite is occasionally replaced by arsenopyrite (FeAsS), where patches of arsenopyrite are seen in the pyrite crystals (Fig. 7e). Inclusions of galena (PbS) are observed in some pyrite crystals. Next in frequency to pyrite is the arsenopyrite where euhedral rhombic crystals pleochroic from gray to white are observed. The other subordinate sulfides; sphalerite (Zn,Fe)S, and galena PbS occur as inclusions while chalcopyrite (CuFeS<sub>2</sub>) forms separate euhedral cubic crystals. The previously described polymetallic sulfides assemblage is characterized by vein-type gold deposit (Fig. 7f).

Harraz (2000) described early and late stages of Au development. He also mentioned that the sulfide minerals are formed in association with the two stages of quartz formation. The sulfide minerals contain gold as inclusions. Using fluid inclusion technique and stable isotope analyses, Harraz (2000) concluded that the Au has been transported as a bisulfide complex. Sharara and Vennemann (1999) and Harraz (2000) concluded that the country rocks on both sides of the veins reflect intensive water/rock interactions by which mesothermal, H<sub>2</sub>O- rich fluids with high concentrations of dissolved As, Au, S and CO<sub>2</sub> introduced into the wall rocks, including destruction of the Fe-, Mg-, and Ca-bearing minerals and deposition of quartz, sericite, albite, muscovite, pyrite, pyrrhotite, calcite and chlorite.

## GEOCHEMISTRY

Fifteen chemical analyses were carried out on the ophiolitic rocks (metamorphic peridotites and metagabbros) and the granitic rocks of Al Fawakhir area to determine their geochemical characteristics. The major and trace elements were analyzed by XRF and spectral techniques to determine the petrogenesis, and the tectonic set-up. Data are shown in Table 2.

### The Metamorphic peridotites:

Plotting the chemical data of Al Fawakhir serpentinites on the CaO, MgO and Al<sub>2</sub>O<sub>3</sub> diagram (Fig. 8), reveal that they occupy field of metamorphic dunite and lherzolite associated with ophiolites defined by Jensen (1976). The samples occupy a restricted area characterized by very low amount of CaO, Al<sub>2</sub>O<sub>3</sub> and higher MgO.

### Metagabbros:

Plotting the chemical analysis data on the SiO<sub>2</sub>-CaO diagram (Fig. 9), which contains two fields; the lower is of low calcium content, while the upper field is of higher CaO content reflecting the amounts of abundance of large mettagabbros cumulate plagioclase phase. The analyzed samples taken from the fine-, medium-, and coarse layers plot in the field of cumulate gabbros on the SiO<sub>2</sub>-CaO binary diagram (Fig. 9). Figure 10 shows the binary relation between SiO<sub>2</sub>% and (Na<sub>2</sub>O%+K<sub>2</sub>O%) Macdonald and Katsura (1964). The plot of the present data shows the theolitic nature of these rocks. All samples plot under the Hawaiiin division line between the alkali and theolitic field.

### Granitic Rocks:

The petrochemical characteristics of the granitic rocks of Al Fawakhir area were determined from major- oxide and trace- element analyses for nine samples. The analyzed samples include all the petrographic varieties. Chemical data and CIPW norms are shown in Tables 3 & 4.

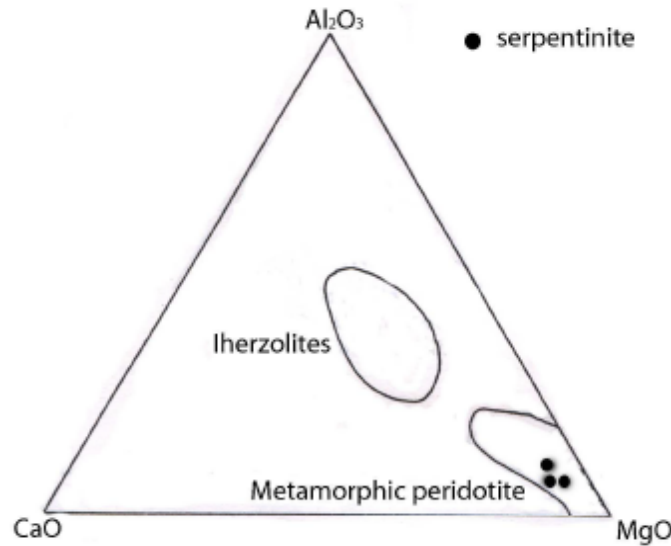


Figure 8. Jensen (1976) diagram showing the composition range of the serpentinite.

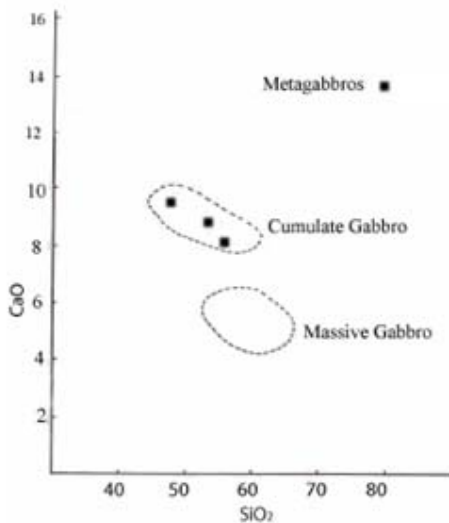


Figure 9. CaO-silica variation diagram for Al Fawakhir metagabbro.

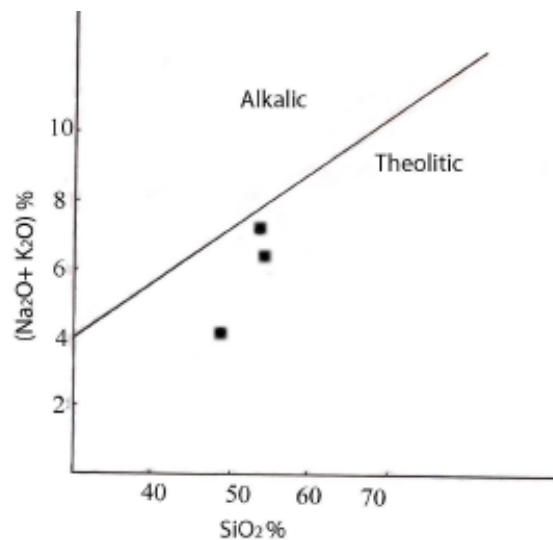


Figure 10. Alkali-silica diagram for Al Fawakhir metagabbro with Hawaiian alkalic and theolitic fields after Macdonald and Katsura (1964).

Figure 11 is after Middlemost (1985) based on the  $\text{SiO}_2$ - total alkalis contents. The present data plot in the granite- field unless the syeno-granites which approach the field of alkali feldspar granites. The Wright's (1969) alkalinity ratio  $[(\text{Al}_2\text{O}_3 + \text{CaO} + \text{alk}) / (\text{Al}_2\text{O}_3 + \text{CaO} - \text{alk})]$  versus  $\text{SiO}_2\%$  variation diagram from Greenberg (1981), Figure 12 shows that the examined granitic rocks can be differentiated into three varieties spread over the subalkaline to alkaline fields.

The  $\text{SiO}_2$  versus  $\text{FeOt} / (\text{FeOt} + \text{MgO})$  wt% variation diagram (Fig. 13) after Maniar and Piccoli (1989) shows that all of the examined granitic rocks fall in the field of the post orogenic granites rift related granites and continental collision granites. Figure 14, after Condie (1973) indicates that the examined granites were intruded in a thick crust (20-30 km). Figure 15 after Pearce et al. (1984),

confirms the previous conclusion on the examined granitic rocks. The plots differentiate between the volcanic arc granite field and the within plate granite field.

The variation diagram of Nb versus Y (Fig. 16) indicates that none of the studied granitic rocks are related to the oceanic ridge granite. The plotted samples distribute over the within-plate granite field and the volcanic arc granite field.

### Summary and conclusions

Al Fawakhir area constitutes a part of the Pan-African belt. It lies in the Eastern Desert of Egypt between latitudes 25°57'00" and 26°00'00" N and longitudes 33°35'00" and 33°38'30" E. Two mines were exploited for gold since the Pharaonic times. These two mines are Al Fawakhir, and El Sid gold mines. Using satellite imagery and aerial photographs, the area is mapped through comprehensive field work. A geologic map (scale 1:40000) is given. The field relations, structural elements and stratigraphic lithology are described and have been discussed during the present work. Samples were collected for Petrographic and petrochemical studies. Geologic mapping revealed that the area is dominantly covered by metamorphic peridotites (serpentinite), metagabbros, granitic rocks, Dokhan Volcanics and forcefully intruded by doleritic dykes and gold-bearing quartz veins. The granitic complex consists of three phases of intrusions; the syenogranites, monzogranites, and alkali feldspar granites.

All samples of these phases plot in the field of granitoides formed by crustal fusion, on the QAP diagram. Hybrid rocks between the granites and the metagabbros. Geochemical analyses, petrochemical parameters, and plotting on the international binary and ternary diagrams revealed that the metamorphic peridotites (serpentinites) belong to the metamorphic dunite, and lherzolite associated with ophiolites. The metagabbros are of tholeiitic nature and are of the cumulate type. The granitic rocks are of subalkaline to alkaline nature. None of the granitic samples are oceanic plagiogranite Al Fawakhir granites are post orogenic, rift-related, and continental collision, intruded within a thick crust (20-30 km).

Table 2: Chemical composition (wt. %) of Al Fawakhir ophiolitic rocks.

	Metamorphic peridotites			Metagabbros		
	1	2	3	1	2	3
SiO <sub>2</sub>	39.69	42.63	39.54	47.87	53.10	54.70
Al <sub>2</sub> O <sub>3</sub>	1.16	0.71	1.14	13.09	14.45	14.18
Fe <sub>2</sub> O <sub>3</sub>	7.75	5.53	7.56	6.73	3.32	4.48
FeO	0.29	1.12	0.25	3.85	4.92	3.54
MgO	37.8	37.05	36.33	12.14	4.80	5.77
CaO	2.45	0.52	0.43	9.67	8.77	6.92
Na <sub>2</sub> O	0.10	0.33	0.10	2.22	4.58	4.33
K <sub>2</sub> O	0.15	0.20	0.16	2.05	2.47	2.44
TiO <sub>2</sub>	0.47	0.15	0.14	0.77	1.53	0.89
MnO	0.17	0.09	0.13	0.16	0.12	0.12
P <sub>2</sub> O <sub>5</sub>	0.20	0.20	0.15	0.17	0.23	0.48
Cr <sub>2</sub> O <sub>3</sub>	0.16	0.17	0.16	-	-	-
H <sub>2</sub> O <sup>-</sup>	7.88	10.59	13.89	1.35	1.27	1.66
H <sub>2</sub> O <sup>+</sup>	1.33	1.08	1.36	0.20	0.17	0.17
Total	99.60	100.36	101.36	100.27	99.74	99.68

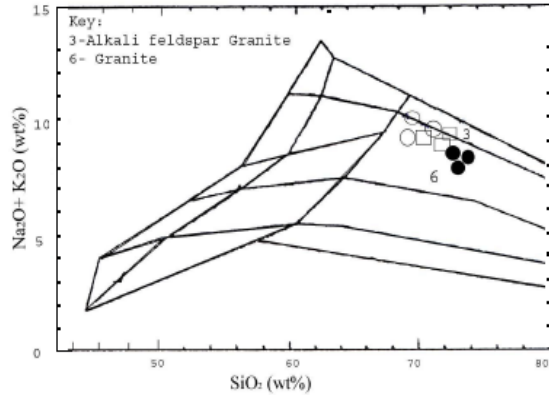


Figure 11. Al Fawakhir granitic rock on the classification diagram of Middlemost (1985).

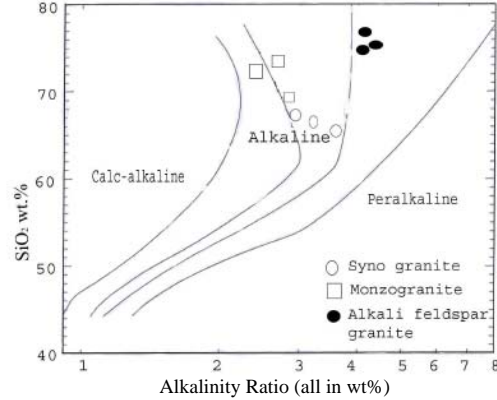


Figure 12. Alkalinity ratio vs silica (wt%) for discrimination among calc-alkaline, alkaline and peralkaline rock suits. Discrimination boundaries after Greenberg (1981).

Alkalinity Ratio (Wright, 1969) =  $(Al_2O_3 + CaO + Na_2O + K_2O) / (Al_2O_3 + CaO - Na_2O - K_2O)$

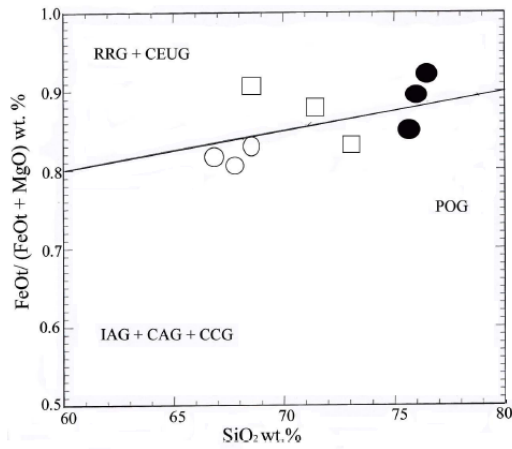


Figure 13.  $SiO_2$  versus  $FeOt / (FeOt + MgO)$  wt% variation diagram after Maniar and Piccoli (1989).

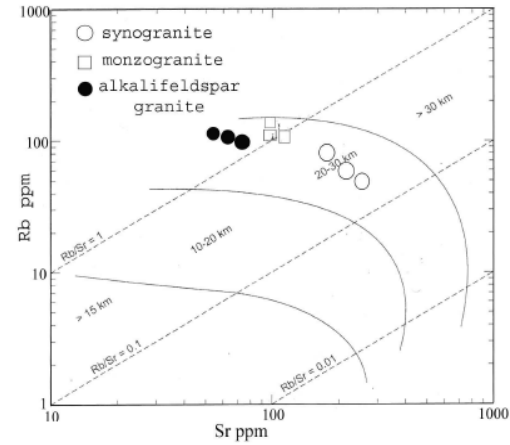


Figure 14. Rb/Sr diagram (after Condie, 1973).

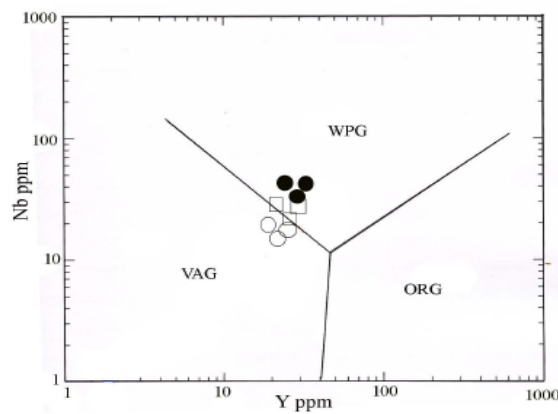


Figure 15. Y vs Nb diagram for granites (after Pearce et al., 1984).

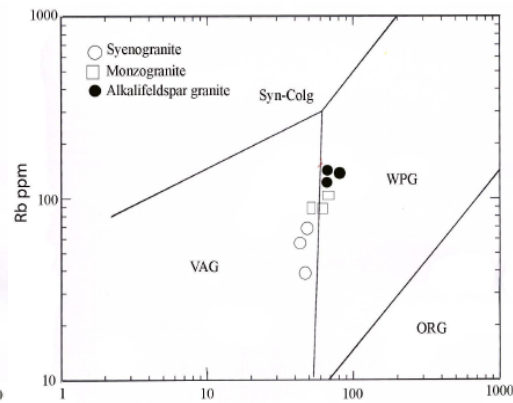


Figure 16. Rb vs (Y+Nb) variation of the granite (after Pearce et al., 1984).

**Table 4: Chemical composition of Al Fawakhir granitic rocks. Data are given in wt.%, unless otherwise stated.**

Rock type	Syeno-granite			Monzo-granite			Alkali feldspar granite		
	1	2	3	4	5	6	7	8	9
SiO <sub>2</sub>	66.36	66.25	66.45	68.29	71.07	72.20	76.30	75.86	76.74
TiO <sub>2</sub>	1.23	0.99	0.33	0.20	0.22	0.24	0.08	0.10	0.05
Al <sub>2</sub> O <sub>3</sub>	14.81	14.65	14.95	15.58	14.18	14.06	12.26	12.06	12.47
Fe <sub>2</sub> O <sub>3</sub>	2.82	3.67	2.65	1.07	1.15	0.49	0.74	0.83	0.65
FeO	0.31	0.72	0.84	1.80	1.45	1.55	0.31	0.32	0.32
MgO	0.71	0.88	0.92	0.27	0.42	0.43	0.13	0.18	0.08
CaO	1.17	2.26	1.83	1.54	1.40	1.39	0.63	0.70	0.56
Na <sub>2</sub> O	3.55	3.02	4.22	4.32	3.89	4.05	3.74	3.80	3.68
K <sub>2</sub> O	6.02	5.33	5.42	5.65	4.84	4.53	4.67	4.48	4.54
MnO	0.21	0.32	0.41	0.06	0.05	0.05	0.03	0.05	0.02
P <sub>2</sub> O <sub>5</sub>	0.05	0.07	0.06	0.06	0.10	0.07	0.06	0.06	0.07
H <sub>2</sub> O <sup>+</sup>	0.64	0.72	0.66	0.90	0.81	0.86	0.50	0.60	0.36
H <sub>2</sub> O <sup>-</sup>	1.12	1.32	1.29	0.87	0.79	0.22	0.49	0.59	0.50
Total	100.00	99.88	100.03	100.61	100.40	100.14	99.96	99.64	99.91
Rb ppm	50	69	80	135	82	108	120	90	110
Ta ppm	1.00	1.20	1.30	2.00	1.60	1.80	2.40	2.60	2.90
Hf ppm	4.20	5.00	6.00	8.00	7.00	6.50	4.00	3.80	3.50
Sr ppm	208	190	200	108	164	113	95	81	83
Nb ppm	18	20	17	20	23	22	26	25	27
Y ppm	28	24	23	34	30	32	43	40	39

**Table 5: Normative Composition of Al Fawakhir granitic rocks.**

Granite type	Syeno-granite			Monzo-granite			Alkali feldspar granite		
Samples	1	2	3	4	5	6	7	8	9
Q	16.00	22.49	18.53	19.98	24.50	26.81	33.39	33.40	34.80
Or	32.62	32.25	36.80	33.70	29.10	27.11	28.15	27.15	23.00
Ab	38.60	27.75	33.00	39.16	35.55	36.85	34.25	35.00	33.65
An	5.94	10.90	5.65	7.3	6.38	6.54	2.75	2.70	2.35
Mt	2.25	0.36	0.00	4.36	1.21	0.51	0.63	0.65	0.69
En	2.58	2.48	2.02	0.74	1.20	1.2	0.40	0.50	0.22
Wo	1.16	0.05	0.00	0.00	0.00	0.00	0.00	0.16	0.00
Il	0.46	1.4	0.84	0.28	0.3	0.34	0.11	0.14	0.07
Ht	0.38	2.38	2.03	0.00	0.00	0.00	0.10	0.16	0.00
Ap	0.125	0.149	0.10	0.12	0.21	0.16	0.12	0.13	0.15
Co	0.00	0.00	0.51	0.00	0.27	0.14	0.00	0.00	0.73
Ru	0.00	0.00	0.46	0.00	0.00	0.00	0.00	0.00	0.00
Fes	0.00	0.00	0.00	0.00	1.25	1.83	0.00	0.00	0.01

## REFERENCES

- Afia, M.S., 1984: History of mining in The Arab World. The Public Egyptian Authority of Books, Egypt, 489 p.
- Akaad, M. K. and El Ramly, M. F., 1960: Geological history and classification of the basement rocks of the Central Eastern Desert of Egypt. Geol. Surv. Egypt, pp. 9-24.
- Andresen, A., Abu El-Rus, M.A., Myhre, P.I., Boghdady, G.Y. and Corfu, F., 2009: U–Pb TIMS age constraints on the evolution of the Neoproterozoic Meatiq Gneiss Dome, Eastern Desert, Egypt, Int. J. Earth Sci. (Geol Rundsch), 98: 481–497.
- Beniamin, N. Y, Youssef, G. M., Azam, G. H., Mahmoud, G. M., Salama , G. A., and Abdel Migid, G. A., 2005: On the mass tectonic Fractures of Northern and Central Eastern Desert, Egypt. Ministry of Petroleum. Internal Report.
- Bonin, B., 1980: Les complexes acides alcalins an orogeniques continentaux: L' exemple de la corse. Ph.D. Thesis Univ. Paris VI, 756p.
- Boulgatov, A. N., Vmarov, M., and Revasov, A. B., 1980: Report on the results of the prospecting work for gold in Al Sid- Semna area. Egyptian Geol. Survey and Mining Authority. Internal Report, 63 p.
- Botros, N. S, 2004: A new classification of the gold deposits of Egypt. Ore Geol. Rev., 25: 1 –37.
- Condie, K.C., 1973, Archean magmatism and crustal thickening, Geol. Soc. of America, Bull., 84: 2981-2992.
- El Gaby, S., 1983: Architecture of the Egyptian basement complex. Proc. 5<sup>th</sup> Int. Conf. Basement Tectonics, Cairo.
- Enoch, J.M., 1999: First known lenses originating in Egypt about 4,600 years ago, Documenta Ophthalmologica, 99: 303-314.
- Greenberg, J.K., 1981: Characteristics and origin of Egyptian younger granites; Summary. Geological Society of America, Bull. 92: 224-232.
- Hashad, A. H., 1980: Present status of geochronological data on the Egyptian basement complex. In: Al Shanti, A.M.S., ed., Evolution and mineralization of the Arabian- Nubian Shield, King Abdulaziz Univ. Jeddah, Bull. 3, Pergamon Press, Oxford, pp. 31-46.
- Hassan, M. A. and Hashad, A. H., 1990: Precambrian of Egypt In: Said, R. ed., The geology of Egypt, Balkema, Rotterdam, Brookfield, pp. 201-245.
- Harraz, H. Z., 2000: A genetic model for a mesothermal Au deposit: evidence from fluid inclusions and stable isotopic studies at El Sid gold mine, Eastern Desert, Egypt, Journal of African Earth Sciences, 30: 267-282.
- Harraz, H. Z.; Hassanen, M. A. and El Dahhar, M.A., 1992: Fluid inclusions and stable isotopic studies at El Sid gold mine, Eastern Desert, Egypt. J. Geol. 36: 243-332.
- Hassanien, S.M.M., 1978: Petrographical and geochemical studies of Gebel Alam-Gebel Umm Khariga basement rocks, Eastern Desert, Egypt. M.Sc. Thesis, Faculty of Sci. Cairo Univ. 134 p.
- Hume, W. F., 1935: Geology of Egypt, Vol. II, Part II Geol. Surv. Egypt.
- Hume, W. F., 1937: Geology of Egypt, V. II. Part III, Geol. Surv. Egypt.
- Jensen, L.S., 1976: A new cation plot for classifying sub-alkaline volcanic rocks. Ontario Dept. Mines, paper 66, 22 p.

- Klemm, D.; Klemm, R. and Murr, A., 2001: Gold of the Pharaohs—6000 year of gold mining in Egypt and Nubia. *Journal of African Earth Sciences*, 33: 643–659.**
- Kochin, G. G. and Bassyuni, F. A., 1968: Mineral resources of the U.A.R., Part I Metallic minerals. Internal Report, Geol. Surv. Egypt, Cairo.**
- Lameyre, J. and Bowden, P., 1982: Plutonic rock types series discrimination of various granitoid series and related rock. *J. Volc. Geotherm. Res.*, 14: 196-86.**
- Macdonald, G.A. and Katsura, T., 1964: Chemical composition of Hawaiian lavas: *J. Petrol.*, 5: 82-132.**
- Maniar, P.D., and Piccoil, P.M., 1989: Tectonic discrimination of granitoids, *Geol. Soc. of America, Bull.*, 101: 635-643.**
- Meneisy, M. Y., 1972: On the isotopic dating of the Egyptian basement rocks. *Annals Geol. Surv. Egypt*, 2: 103-1097.**
- Meneisy, M.Y. and Lenz, H., 1982: Isotopic ages of some Egyptian granites, *Annals Geologic Survey Egypt*, 12: 7-14.**
- Middlemost, E.A.M., 1985: Magmas and magmatic rocks: An introduction to igneous peterology. Longman. Inc., New York, 266 p.**
- Moussa, E.M.M., Stern, R.J., Manton, W.I., Kamal, A.A., 2008: SHRIMP zircon dating and Sm/Nd isotopic investigations of Neoproterozoic granitoid, Eastern Desert, Egypt. *Precambrian Res.*, 160: 341-356.**
- Pearce, J.A., Nigel, P.W., and Andrew, 1984: Trace elements discrimination diagrams for tectonic interpretation of granitic rocks, *Journal of Petrology*, 35: 956-983.**
- Sharara, N., and Venneman, T.W., 1999: Composition and origin of the fluid responsible for gold mineralization in some occurrences in the Eastern Desert, Egypt: Evidence from fluid inclusions and stable isotope; 1<sup>st</sup> International Conf. of the Geol. of Africa, I: 421-445.**
- Streckeisen, A.L., 1967: Classification and nomenclature of igneous rocks. *Neues Jahrb. Mineral. Abh.*, 107: 144-240.**
- Wright, J.B., 1969: A simple alkalinity ratio and its applications to questions of non- orogenic granitic- gneisses. *Geol. Mag.*, 46: 1097-1111.**